The paper was published in the proceedings of the 11th International Conference on Physical Modelling in Geotechnics (ICPMG2026) and was edited by Ioannis Anastasopoulos. The conference was held from June 8th to June 12th 2026 in Zurich, Switzerland.

Proceedings of the 11th ICPMG 2026
11th International Conference on Physical Modelling in Geotechnics
8-12 June 2026, Zurich, Switzerland

Centrifuge model tests on buried pipe uplift in liquefied ground using in-situ soil

H.K. Hong and T. Tobita
Kansai University, Suita, Japan, k561984@kansai-u.ac.jp, tobita@kansai-u.ac.jp

ABSTRACT: This study conducted centrifuge model tests on the liquefaction-induced uplift of underground pipes using Toyoura standard sand and in-situ sand collected from Uchinada, Ishikawa Pref., Japan. The study focuses on two aspects: (1) a comparative investigation of the uplift behaviour of buried pipes with and without countermeasures in Toyoura sand and in-situ Uchinada sand, and (2) the proposal of a reuse approach for methylcellulose-mixed viscous-fluid-saturated soil in centrifuge tests. The experimental results show that the uplift of pipes without countermeasures in Uchinada sand was significantly greater than that in Toyoura sand. When countermeasures were applied, pipe uplift in Toyoura sand was effectively suppressed to near zero, whereas non-negligible uplift was still observed in Uchinada sand. This difference was attributed to the lower shear strength of Uchinada sand, indicating that countermeasures proven effective in standard sand may not fully prevent damage in other soil types. These findings further underscore the need to investigate combined mitigation strategies, such as ground reinforcement, rather than relying on a single countermeasure. Given the limited availability of in-situ Uchinada sand, this study presents a reuse method based on the thermal gelation property of methylcellulose, enabling the recycling of viscous fluid-saturated soil in centrifuge experiments.

1 INTRODUCTION

Earthquake-induced liquefaction is a geotechnical hazard that causes ground deformation and infrastructure damage. Underground pipelines are particularly vulnerable to liquefaction-induced ground deformation and have suffered repeated failures during major seismic events, such as the Northridge earthquake in 1994 (Lau et al., 1995), the Chi-Chi earthquake in 1999 (Yu et al., 2001), the Christchurch earthquake in 2011 (Cubrinovski et al., 2011), and the Tohoku earthquake in 2011 (Yasuda et al., 2013).

Liquefaction is characterised by a seismic-induced increase in pore water pressure and a corresponding reduction in effective stress, leading the ground to behave like a fluid. As a result, buried pipes may be uplifted by buoyant forces generated by the liquefied soil.

To clarify pipe uplift behaviour, numerous experimental and numerical studies have been conducted (e.g., Koseki et al., 1997, 1998; Chian and Madabhushi, 2012; Chian et al., 2014). Also, various countermeasures have been proposed, including weight structures, grouting, gravel replacement, drainpipes, and horizontal plates (Towhata et al., 2015; Otsubo et al., 2016; Castiglia et al., 2019; Ecemis et al., 2021; Hong et al., 2024a). However, complete suppression of pipe uplift has not been consistently achieved, and potential adverse effects associated with existing countermeasures have been reported (Hong et al., 2024a, b).

Centrifuge model experiments have been regarded as a practical approach for evaluating soil liquefaction, as they enable examination under stress states representative of prototype conditions through centrifugal acceleration (Madabhushi, 2017). To satisfy the permeability and time-scaling requirements in such experiments, viscous fluids are commonly used to achieve soil saturation. While this approach facilitates reliable simulation of liquefaction behaviour, it introduces practical limitations, as soils saturated with viscous fluids are generally difficult to reuse when the available quantity of soil is limited.

Present study aims to identify an effective countermeasure for mitigating pipe uplift and to verify its performance through centrifuge model tests using Toyoura standard sand and in-situ soil collected from a site severely affected by liquefaction during the 2024 Noto Peninsula, Japan, earthquake. In addition, to address the practical constraint of limited soil availability in viscous-fluid-saturated centrifuge experiments, this study proposes a method for reusing viscous-fluid-saturated soil, thereby enhancing experimental flexibility and cost efficiency.

2 METHODS

2.1 Centrifuge experiment

Centrifuge model experiments were performed at the Kansai University centrifuge facility in Japan with a 50 G condition. The experiments utilised a rigid box with internal dimensions of 45 cm in length, 20 cm in width, and 40 cm in height.

The soil materials used in this study are summarised in Table 1 and consist of Toyoura sand as a reference material and in-situ soil collected near Nishiaraya Elementary School in Uchinada following the 2024 Noto Peninsula earthquake. The grain size distribution curves of the soils are shown in Figure 1, and the sampling location of the in-situ soil is presented in Figure 2. The sampling site experienced severe liquefaction-induced lateral spreading, with ground displacements exceeding 2 m in some locations, as documented in the ground deformation survey shown in Figure 3 (Hasshu Co., Ltd., 2024).

Table 1. Material properties of Toyoura sand and Uchinada sand.

Properties	Toyoura	Uchinada
Specific gravity G_s	2.66	2.65
Min void ratio e_{min}	0.62	0.65
Max void ratio e_{max}	0.94	0.96
Max dry density ρ_{max} (Mg/m^3)	1.64	1.61
Min dry density ρ_{min} (Mg/m^3)	1.37	1.36
Median particle size D_{50} (mm)	0.11	0.15

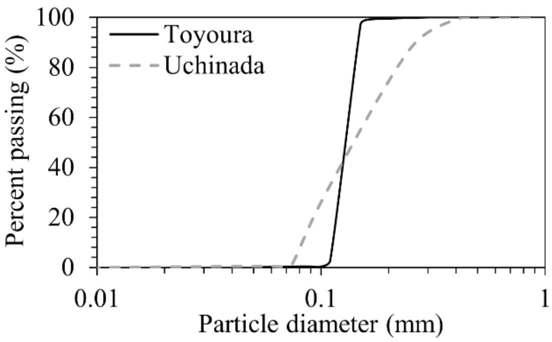

Figure 1. Grain size distribution curves of Toyoura sand and in-situ soil (Uchinada sand).

Figure 2. Soil Sampling Location (Google Maps).

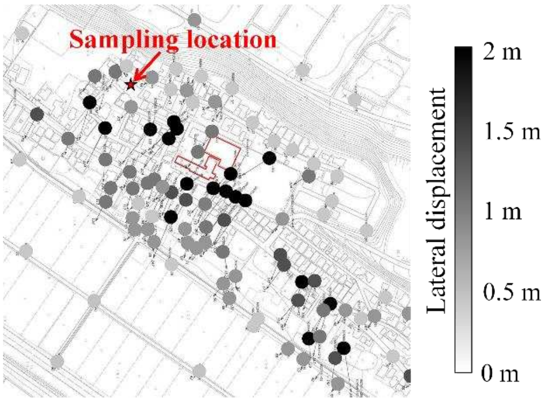

Figure 3. The ground displacement after 2024 Noto Peninsula earthquake (Hasshu Co., Ltd. (2024)).

Figure 4 shows the experimental model configuration. The pipe was buried at an H/D ratio of 1, where H is burial depth and D is pipe diameter. Ground models were prepared by air pluviation targeting a medium relative density (D_r) of 60%. As a result, the ground models were formed with a relative density of 64% for Toyoura sand and 70% for the in-situ Uchinada soil. All ground models were saturated with viscous fluid with a kinematic viscosity of 50 cSt (Shin-Etsu Chemical Co., Ltd., 2005).

Two types of pipe models were considered for both Toyoura sand and Uchinada soil: a no-countermeasure (NC) pipe and a pipe equipped with a bottom plate countermeasure (BPC) attached to the bottom of the pipe. Photographs of the NC pipe and the BPC pipe models used in the experiments are shown in Figure 5. The density of the pipe is 0.3 Mg/m^3, and that of the horizontal plate is 1.17 Mg/m^3.

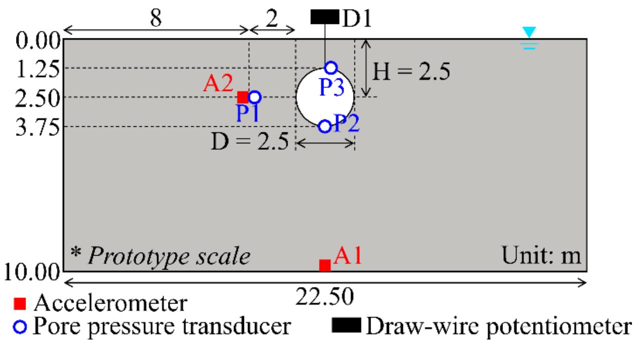

Figure 4. Schematic diagram of the experimental model.

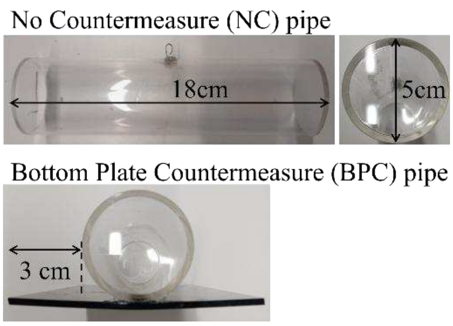

Figure 5. Experimental pipe models.

Figure 6 presents the input acceleration applied in the centrifuge experiment (a) and the recorded ground accelerations from the 2024 Noto Peninsula earthquake at the K-NET observation station, ISKH08, closest to Nishiaraya Elementary School, located approximately 12.9 km away [(b) East-West (EW), (c) North-South (NS), and (d) Up-Down (UD)] (NIED).

Although the present experiments aim to capture key characteristics of the phenomena observed during the 2024 Noto Peninsula earthquake, the actual earthquake motion has a longer duration than can be reproduced by the hydraulic shaking table of the centrifuge apparatus. Therefore, the experimental input acceleration was designed to be comparable to the cumulative Arias intensity (I_A) obtained by summing the EW, NS, and UD components of the recorded earthquake motion.

The experimental cases are listed in Table 2.

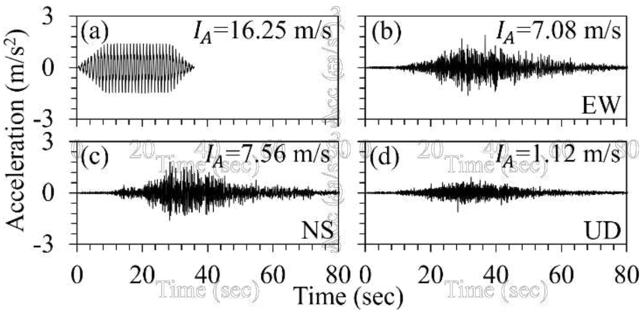

Figure 6. Comparison of the (a) experimental input acceleration and the (b)-(d) recorded ground motions of the 2024 Noto Peninsula earthquake (K-NET, ISKH08, NIED).

Table 2. Experimental cases.

Case ID	Soil material (D_r)	Pipe type
NC_T	Toyoura sand (64%)	NC pipe
BPC_T	Toyoura sand (64%)	BPC pipe
NC_U	Uchinada sand (70%)	NC pipe
BPC_U	Uchinada sand (70%)	BPC pipe

After the centrifuge experiments, a soil-cleaning process was conducted to remove the viscous methylcellulose fluid and enable reuse of the soil material. The cleaning procedure was designed to remove methylcellulose from the viscous fluid-saturated soil while preventing the loss of fine particles. Approximately 17,000 cm^3 of soil was subjected to the cleaning process after each experimental case. Soil washing was performed using a rotating agitation device in a cylindrical container with a volume of 78,000 cm^3. This container size was selected to allow sufficient water to be added, ensuring adequate dilution of methylcellulose during the cleaning process. After washing, the soil-water mixture was dried in an air-drying oven of 75 cm in width, 58 cm in depth, 100 cm in height (Marui & Co., Ltd.).

3 RESULTS

3.1 Centrifuge experiments

In this section, the experimental results are presented together with their physical interpretation to facilitate a clear understanding of the observed phenomena.

Figure 7 compares the experimental results obtained using Toyoura sand for the NC and BPC pipes (Cases NC_T and BPC_T). Uniform input accelerations (A1) were applied in both cases. However, attenuation of acceleration amplitude in the surrounding ground (A2) was more pronounced in the BPC pipe.

EPWP results also differed between the two cases. At the pipe's top (P3), bottom (P2), and in the surrounding ground (P1), larger EPWP were observed for the BPC pipe than for the NC pipe. Here, the effective stress can change rapidly due to pipe uplift, making meaningful comparison with the initial effective stress (σ'_0) valid only in the free field (P1). Notably, EPWP at P1 exceeded the initial effective stress in the BPC case. Despite the larger reduction in ground strength in the BPC case, the pipe uplift was limited to only 2.5 cm, compared with 17.75 cm in the NC case, indicating that the BPC reduced pipe uplift to approximately 14% of that observed for the NC pipe.

Figure 8 shows the results on in-situ Uchinada sand cases (Cases NC_U and BPC_U). Input accelerations (A1) are similar to those described above. In the surrounding ground (A2), attenuation of acceleration amplitude was more pronounced for the BPC pipe, consistent with the trends observed in the Toyoura sand case. However, ground motion toward the pipe direction (negative direction) was slightly more constrained than in the Toyoura sand case. The pipe uplift (D1) reached 22.25 cm for the NC pipe and 7.0 cm for the BPC pipe, corresponding to approximately 1.25 and 2.8 times those observed in the Toyoura sand case, respectively.

For the NC pipe in in-situ Uchinada sand, EPWP measured at both the pipe's top (P3) and bottom (P2) showed an increasing trend, unlike the Toyoura sand case. A reduction in EPWP was observed only at the pipe's top after sufficient pipe uplift. For the BPC pipe, a slight negative EPWP was observed at the pipe's top during the early stage of pipe uplift, followed by a relatively limited increase compared with that observed in Toyoura sand. In contrast, EPWP at the pipe's bottom increased more rapidly than in the Toyoura sand case. In the surrounding ground (P1), EPWP increased more significantly for the NC pipe, whereas the increase in EPWP for the BPC pipe was less pronounced than that observed in Toyoura sand.

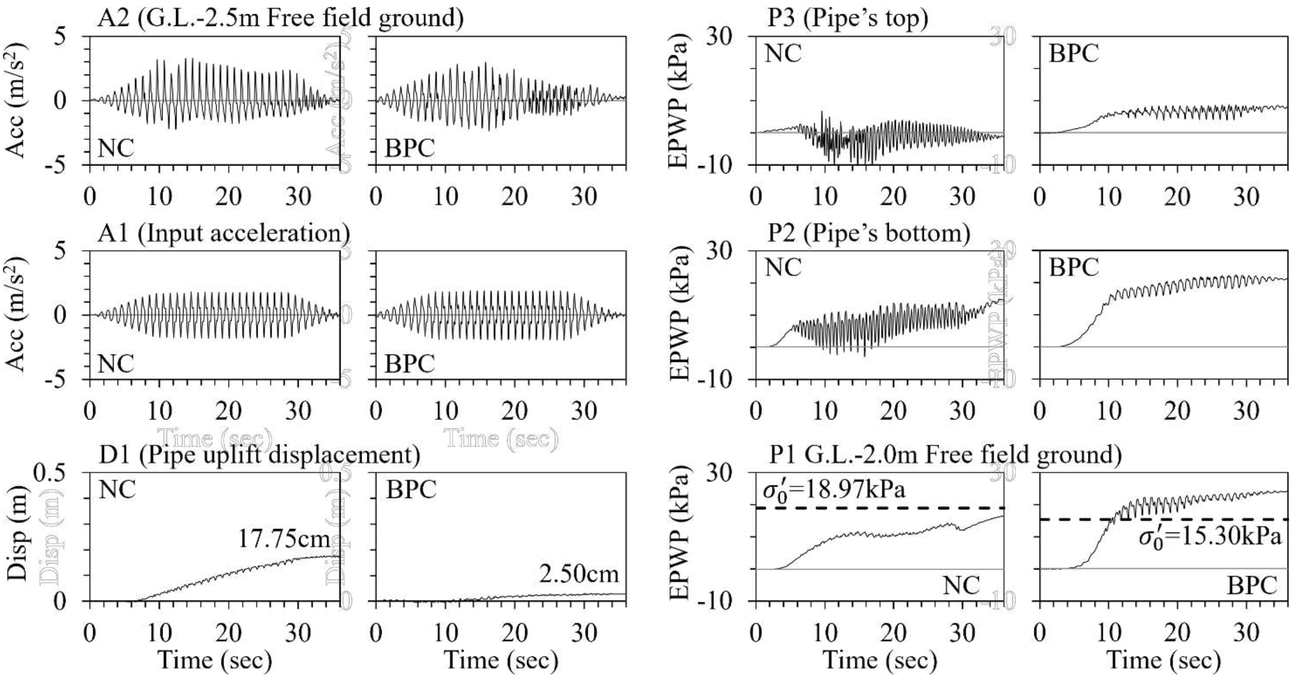

Figure 7. Experimental results for NC and BPC pipes in Toyoura sand.

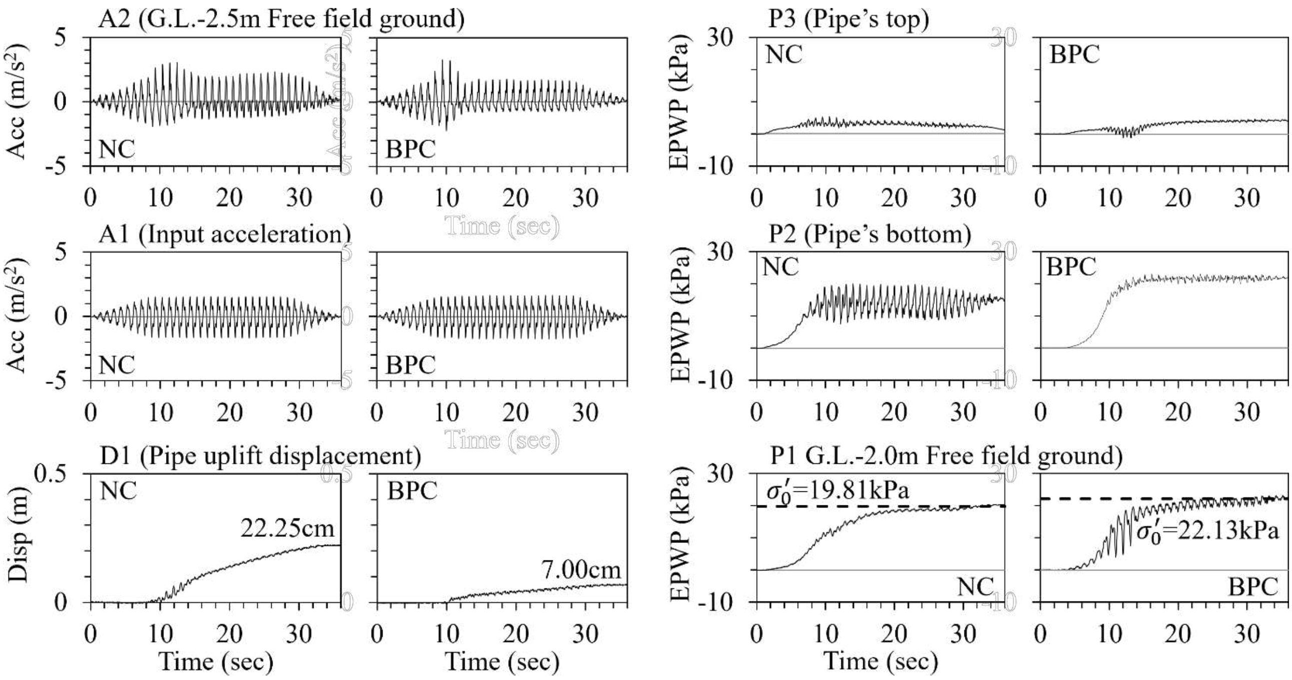

Figure 8. Experimental results for NC and BPC pipes in in-situ Uchinada sand.

In Toyoura sand cases, the pipe uplift prevention mechanism of the BPC can be explained by the role of the soil above the plate, which acts as a counterweight resisting pipe uplift and contributes to the expansion of the mobilised shear resistance plane, as illustrated in Figure 9. However, under liquefied conditions, the reduction in effective stress significantly diminishes shear resistance. Therefore, the increase in the weight of the overlying soil becomes the primary mechanism governing the uplift resistance provided by the BPC.

Paradoxically, this uplift-prevention mechanism is supported by the observation that liquefaction of the surrounding ground was more pronounced in the BPC pipe case than in the NC pipe case. Specifically, greater attenuation of acceleration amplitude (A2) and a more pronounced increase in EPWP were observed in the soil surrounding the BPC pipe than in that surrounding the NC pipe (P1). These responses indicate that the uplift force acting on the pipe was transferred to the surrounding soil through the plate, resulting in additional pressure on the adjacent ground.

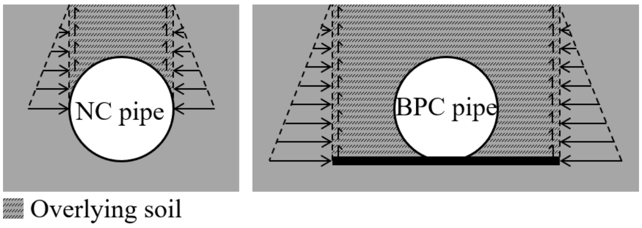

Figure 9. Pipe uplift resist mechanism of the BPC.

Furthermore, unlike the NC pipe, the soil at the top (P3) and bottom (P2) of the pipe in the BPC case did not undergo volumetric expansion associated with pipe uplift. Since volumetric expansion reduces EPWP, its absence in the BPC case resulted in higher EPWP at both the top and bottom of the pipe. In contrast, for the NC pipe, volumetric expansion induced by pipe uplift was observed at both locations, accompanied by a reduction in EPWP.

The measured uplift of 2.50 cm for the BPC pipe in Toyoura sand corresponds to 1 mm at the model scale. This is comparable to potential measurement artifacts arising from realignment of the connection between the pipe and the draw-wire potentiometer, as well as lateral displacement induced by the input acceleration rather than actual vertical uplift. Therefore, the BPC can be regarded as having effectively suppressed pipe uplift to nearly zero in the Toyoura sand case.

Since the uplift mitigation mechanism of the BPC is based on a substantial increase in the resisting weight of the soil above the pipe, together with the expansion of the shear resistance plane mobilised above the plate, it is inherently effective under shallow burial conditions, where resistance to pipe uplift is otherwise limited due to low overburden pressure and shear resistance of the overlying soil.

In contrast, although the BPC reduced pipe uplift in the in-situ Uchinada sand case, the uplift did not converge to near-zero as observed in the Toyoura sand case, despite the higher relative density of the Uchinada sand (70%) compared with that of the Toyoura sand (64%).

Unlike the Toyoura sand cases, an apparent reduction in EPWP at the pipe top and bottom was not observed for the NC pipe in Uchinada sand. This indicates that, despite the larger pipe uplift observed in the Uchinada sand case compared with the Toyoura sand case, the volumetric expansion of the soil surrounding the pore pressure transducers associated with pipe uplift was minimal. This behaviour is interpreted to result from the localisation of shear deformation above the pipe during uplift. It should be noted that this interpretation is based on indirect evidence from sensor measurements, as direct observation of soil deformation at the top of the buried pipe during uplift was not possible in the present experiments. Such localised shear deformation is considered to be associated with the lower internal friction angle of Uchinada sand, reported to be approximately 35 degrees (GEER, 2024), compared with that of Toyoura sand (approximately 42 degrees) (Hatanaka and Uchida, 1996). Localised shear deformation may also have occurred in the BPC cases, which is interpreted as a factor contributing to the reduced effectiveness of the BPC in suppressing pipe uplift in Uchinada sand.

The present results indicate that the BPC is more effective than existing countermeasures at mitigating pipe uplift. However, experiments using in-situ Uchinada sand suggest that even the BPC may not completely prevent pipe uplift, depending on ground characteristics. Therefore, for soft sandy soils such as Uchinada sand, additional countermeasures, including ground reinforcement, may be required in combination with the BPC to prevent liquefaction-induced pipe uplifts during earthquakes.

3.2 Reusability of viscous-fluid-saturated soil

The centrifuge experimental results indicate that additional centrifuge experiments and element-scale tests are required to further clarify the behaviour of Uchinada sand. Such additional investigations inevitably require a substantial amount of soil material, highlighting the importance of reusing in-situ sand, which is generally available only in limited quantities. While soil reuse is relatively straightforward in conventional laboratory tests involving water saturation followed by oven drying, centrifuge experiments commonly employ viscous fluids for soil saturation to satisfy permeability and time-scaling requirements. As a result, the reuse of soil material after centrifuge experiments becomes challenging. In particular, removing viscous fluids while preserving the original soil characteristics, especially without inducing the loss of fine particles, remains a critical issue.

Figure 10 schematically illustrates the overall procedure for removing the viscous fluid, while Figure 11 provides representative photographs to aid visual understanding of the cleaning process. After the centrifuge experiments, approximately 17,000 cm^3 of saturated soil from the rigid box was transferred to a bucket (78,000 cm^3) and mixed well with tap water using a rotary agitator [Figure 10(1)]. Through this process, a substantial portion of the methylcellulose adhering to the soil particle was diluted. Specifically, although the initial kinematic viscosity of the pore fluid was 50 cSt, mixing with a large amount of tap water reduced it to approximately 2 cSt, indicating that the pore fluid was already substantially diluted when compared with tap water, which has a kinematic viscosity of roughly 1 cSt.

Turbidity caused by fine particles in the Uchinada sand persisted after 24 hours, as shown in Figure 11(a). The fluid, mixed with a diluted methylcellulose solution and fine particles, was transferred to a steel container by applying a hydraulic head difference using a towel filter [Figure 10(2)]. The towel was a regular shower towel and could not completely prevent the migration of fine particles into the steel container. The fluid was then placed in a drying oven at 100 °C for 5 hours [Figure 10(3)]. As shown in Figure 11(b), thermally solidified methylcellulose sheets (red circles) remained on the water surface, while the fine particles settled at the bottom of the container.

After removing the solidified methylcellulose and the clean surface fluid, the settled fine particles were washed with water and returned to the bucket, and the same procedure was repeated. Also, the fine particles retained in the towel were washed and returned to the bucket to minimise fine loss. After five repetitions, no solidified methylcellulose was observed, as shown in Figure 11(c). To ensure complete removal of methylcellulose, the procedure was repeated five additional times (total of 10 cycles). After drying all the soil in the bucket, reusable in-situ Uchinada sand was obtained without loss of fine particles, with the methylcellulose effectively removed.

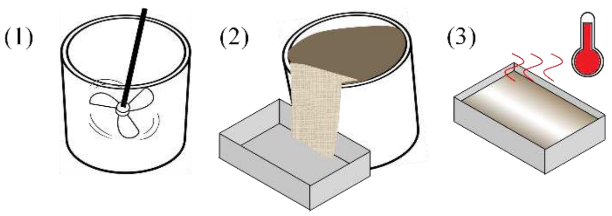

Figure 10. Schematic of the procedure for removing viscous fluid from soil after centrifuge experiments.

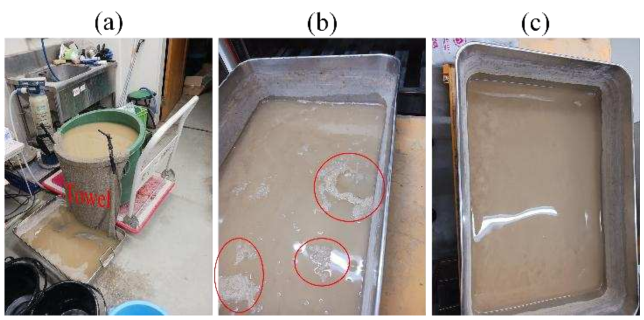

Figure 11. Photographs of the viscous fluid removal process: (a) filtration using a towel, (b) thermally solidified methylcellulose on the water surface, and (c) absence of solidified methylcellulose after repeated cleaning cycles.

Such cleaning procedures become increasingly complex as the fine content of the soil increases. In contrast, standard sands commonly used in liquefaction experiments, such as Toyoura sand and Ottawa sand, which contain negligible fines, are expected to allow effective reuse through considerably simplified procedures.

Due to the time-consuming nature of the cleaning procedure, the results presented in this study do not include experiments conducted using the cleaned soil. To evaluate the effectiveness of the proposed soil reuse approach, further verification is required through element tests comparing the liquefaction characteristics of the cleaned soil with those of the original. Nevertheless, the grain size distribution of the cleaned soil was confirmed to be identical to that of the soil before the experiment (Figure 1).

It should be noted that when fines placed in the drying oven are exposed to surfaces in direct contact with hot air for an extended period, fines may dry in an agglomerated and hardened state. Therefore, during the final drying stage, the soil should be periodically turned over by moving the lower portion to the upper surface to ensure uniform drying and prevent fines from agglomerating. In addition, owing to this characteristic, drying at temperatures below 100 °C is preferable to the commonly adopted 110 °C, unless the water level fully covers the soil surface, as lower drying temperatures are more effective in preventing the agglomeration and hardening of fine particles.

4 CONCLUSIONS

This study investigated liquefaction-induced uplift behaviour of buried pipes through centrifuge model experiments using both Toyoura standard sand and in-situ soil collected from Uchinada, Ishikawa pref., Japan, following the 2024 Noto Peninsula, Japan, earthquake. Particular attention was given to the effectiveness of a bottom plate countermeasure (BPC) and to the practical issue of reusing viscous-fluid-saturated soil in centrifuge experimentation.

Centrifuge experiments using Toyoura sand demonstrated that the BPC was highly effective at suppressing pipe uplift, reducing uplift displacement to near zero. Although acceleration attenuation and excess pore water pressure (EPWP) development around the pipe were more pronounced in the BPC cases than in the no-countermeasure cases, these responses indicated that uplift resistance was effectively mobilised through the increased resisting weight of the soil mass above the plate. Centrifuge experiments using Toyoura sand indicate that enlarging the plate dimensions is expected to enhance anti-uplift performance by increasing the resisting soil mass and the extent of shear resistance mobilisation. However, the mechanism of BPC identified in this study suggests that even small bottom-plate dimensions may be sufficient to suppress pipe uplift. As the influence of bottom-plate dimensions was not systematically investigated in the present study, further experimental and numerical research is necessary to determine the optimal plate size and to generalise the applicability of the BPC.

In contrast, experiments using in-situ Uchinada sand revealed that although the BPC significantly reduced pipe uplift, it did not suppress uplift to near-zero levels, even under a higher relative density than in the Toyoura sand cases. EPWP responses near the pipe showed distinct differences from those observed in Toyoura sand, particularly the absence of an apparent EPWP reduction at the pipe top and bottom associated with volumetric expansion. These results indicate that pipe uplift in Uchinada sand was accompanied by localised shear deformation above the pipe, rather than distributed deformation. This behaviour is attributed to the lower internal friction angle of Uchinada sand compared with Toyoura sand, leading to reduced mobilisation of shear resistance and diminished effectiveness of the BPC. The findings suggest that, while the BPC is a highly effective countermeasure, its performance can be strongly influenced by soil strength characteristics, and that additional ground improvement or reinforcement measures may be required in soft sandy grounds to fully prevent liquefaction-induced pipe uplift.

In addition to the uplift behaviour, this study addressed a practical challenge in centrifuge experiments involving viscous fluids for soil saturation. Since viscous-fluid-saturated soils are generally challenging to reuse, especially when the available in-situ soil quantity is limited, a soil-cleaning and reuse method was proposed. By exploiting the thermal gelation property of methylcellulose, the proposed procedure enables the removal of the viscous fluid without fines loss. It was confirmed that the grain-size distribution remained unchanged after cleaning. The proposed method provides a practical means to overcome limitations on soil quantity and improves the flexibility and cost-efficiency of centrifuge experimentation.

Although sensor-based measurements were successfully conducted for the soft sand (in-situ Uchinada sand) used in this study, a detailed visual analysis of deformation and interaction mechanisms during the pipe uplift process was not possible. Accordingly, further experimental investigations employing advanced modelling techniques and improved instrumentation are required to capture the soil-pipe interaction behaviour more comprehensively.

Furthermore, to enable broader application of soil-reuse methods involving washed soils, comparative evaluations using element-scale liquefaction tests are necessary to assess potential changes in liquefaction characteristics. Additional studies are therefore required to assess the validity and applicability of soil reuse strategies.

ACKNOWLEDGEMENTS

The authors thank the Subcommittee on Rational Earthquake and Tsunami Countermeasures for Water and Sewage Facilities of the Earthquake Engineering Committee, Japan Society of Civil Engineers, for their valuable comments. The first author, Hyuk-Kee Hong, acknowledges the support of the Rotary Club of Toyonaka Minami, Rotary International District 2660.

REFERENCES

Castiglia, M., de Magistris, F. S., Onori, F. and Koseki, J. (2021). Mitigation systems for the uplift of buried pipelines in liquefiable soils under repeated shaking through model tests. *Soil Dynamics and Earthquake Engineering*, 148, 106850. https://doi.org/10.1016/j.soildyn.2021.106850

Chian, S. C. and Madabhushi, S.P.G. (2012). Effect of buried depth and diameter on uplift of underground structures in liquefied soils. *Soil Dynamics and Earthquake Engineering*, 41, pp. 181-190. https://doi.org/10.1016/j.soildyn.2012.05.020

Chian, S. C., Tokimatsu, K. and Madabhushi, S.P.G. (2014). Soil liquefaction-induced uplift of underground structures: physical and numerical modelling. *Journal of Geotechnical and Geoenvironmental Engineering*, 140(10), 04014057. https://doi.org/10.1061/(ASCE)GT.1943-5606.0001159

Cubrinovski, M., Bradley, B., Wotherspoon, L., Green, R., Bray, J., Wood, C., Pender, M., Allen, J., Bradshaw, A., Rix, G., Taylor, M., Robinson, K., Henderson, D., Giorgini, S., Ma, K., Winkley, A., Zupan, J., O'Rourke, T., DePascale, G. and Wells, D. (2011). Geotechnical aspects of the 22 February 2011 Christchurch earthquake. *Bulletin of the New Zealand Society for Earthquake Engineering*, 44(4), pp. 205-226. https://doi.org/10.5459/bnzsee.44.4.205-226

Ecemis, N., Valizadeh, H. and Karaman, M. (2021). Sand-granulated rubber mixture to prevent liquefaction-induced uplift of buried pipes: a shaking table study. *Bulletin of Earthquake Engineering*, 19, pp. 2817-2838. https://doi.org/10.1007/s10518-021-01091-3

GEER Association. (2024). Geotechnical reconnaissance of the 2024 Noto Peninsula Earthquake: Final Report. *Geoengineering Extreme Events Reconnaissance Association*.

Hasshu Co., Ltd. (2024). 2024 Noto Peninsula Earthquake: Survey Report on Ground Deformation Assessment and Measurement of Ground Displacement in Uchinada Town. June 2024. (in Japanese).

Hatanaka, M., and Uchida, A. (1996). Empirical correlation between penetration resistance and internal friction angle of sandy soils. *Soils and foundations*, 36(4), pp. 1-9. https://doi.org/10.3208/sandf.36.4_1

Hong, H. K., Tobita, T., Miyamoto, K. and Konishi, Y. (2024a). Validation of a countermeasure against pipe uplift during liquefaction. *4th Asia-Pacific Conference on Physical Modelling in Geotechnics (ACPMG), Abu Dhabi, UAE*, 11-13 December 2024.

Hong, H. K., Tobita, T., Miyamoto, K. and Konishi, Y. (2024b). Analysis of resistance mechanisms and countermeasures against pipe uplift during liquefaction. *Japanese Geotechnical Society Special Publication*, 10(51), pp. 1912-1917. https://doi.org/10.3208/jgssp.v10.OS-40-03

Koseki, J., Matsuo, O. and Koga, Y. (1997). Uplift behavior of underground strictures caused by liquefaction of surrounding soil during earthquake. *Soils and Foundations*, 37 (1), pp. 97-108. https://doi.org/10.3208/sandf.37.97

Koseki, J., Matsuo, O. and Tanaka, S. (1998). Uplift of sewer pipes caused by earthquake-induced liquefaction of surrounding soil. *Soils and Foundations*, 38(3), pp. 75-87. https://doi.org/10.3208/sandf.38.3_75

Lau, D. L., Tang, A., and Pierre, J. R. (1995). Performance of lifelines during the 1994 Northridge earthquake. *Canadian journal of civil engineering*, 22(2), pp. 438-451. https://doi.org/10.1139/l95-052

Madabhushi, G. (2017). *Centrifuge modelling for civil engineers*. CRC press. https://doi.org/10.1201/9781315272863

Marui & Co., Ltd. (n.d.). Physical properties testing apparatus for soil (Item 15). Retrieved from https://www.marui-group.co.jp/products/soil/physical-test/item-15/

National Research Institute for Earth Science and Disaster Resilience (NIED). https://www.kyoshin.bosai.go.jp/

Otsubo, M., Towhata, I., Hayashida, T., Shimura, M., Uchimura, T., Liu, B., Taeseri, D., Cauvin, B. and Rattez, H. (2016). Shaking table tests on mitigation of liquefaction vulnerability for existing embedded lifelines. *Soils and Foundations*, 56(3), pp. 348-364. https://doi.org/10.1016/j.sandf.2016.04.003

Shin-Etsu Chemical Co., Ltd. (2005). *METOLOSE Brochure*.

Towhata, I., Otsubo, M., Uchimura, T., Shimura, M., Liu, B., Hayashida, T., Taeseri, D. and Cauvin, B. (2015). Shaking model tests on liquefaction mitigation of embedded lifeline. in *Perspectives on Earthquake Geotechnical Engineering: In Honour of Prof. Kenji Ishihara*, pp. 311-341. https://doi.org/10.1007/978-3-319-10786-8_12

Yasuda, S., Towhata, I., Ishii, I., Sato, S., & Uchimura, T. (2013). Liquefaction-induced damage to structures during the 2011 great east Japan earthquake. *Journal of JSCE*, 1(1), pp. 181-193. https://doi.org/10.2208/journalofjsce.1.1_181

Yu, S.B., Kuo, L.C., Hsu, Y.J., Su, H.H., Liu, C.C., Hou, C.S., Lee, J.F., Lai, T.C., Liu, C.C., Liu, C.L. and Tseng, T.F. (2001). Preseismic deformation and coseismic displacements associated with the 1999 Chi-Chi, Taiwan, earthquake. *Bulletin of the Seismological Society of America*, 91(5), pp. 995-1012. https://doi.org/10.1785/0120000722